

Transport and Diffusion Calculations on MRI-generated Data

Andreas H. Hielscher¹, Raymond E. Alcouffe² and Randall L. Barbour³

Los Alamos National Laboratory, Los Alamos, New Mexico 87545

¹Bioscience and Biotechnology, CST-4, MS E535

²Transport Methods, XTM, MS B226

³SUNY Health Science Center of Brooklyn, Department of Pathology
450 Clarkson Ave., Brooklyn, New York 11203

ABSTRACT

In this study we analyze the limits of the diffusion approximation to the Boltzmann transport equation for photon propagation in the human brain. Two dimensional slices through the head are obtained with the method of magnetic resonance imaging (MRI). Based on these images we assign optical properties to different regions of the brain. A finite-difference transport/diffusion code is then used to calculate the fluence throughout the head. Differences between diffusion and transport calculations occur especially in void-like spaces and regions where the absorption coefficient is comparable to the reduced scattering coefficient.

Keywords: Photon propagation in tissues, transport theory, diffusion theory, discrete ordinate, finite difference, brain, magnetic resonance imaging.

1. INTRODUCTION

Light propagation over long distances in biological tissues is commonly approximated as a diffusive process.¹ The widespread acceptance of this approximation is partly based on experimental verification for certain cases²⁻⁵ and partly on the relative simple mathematical structure of diffusion theory. However, it is also known that the diffusion approximation does not hold if the absorption coefficient, μ_a , of the medium is not much smaller than the reduced scattering coefficient, μ_s .^{6,7} In biological tissues this is in general the case when the wavelength used to probe the tissue is shorter than 650 nm or longer than 900 nm. Inside of blood vessels or organs with a high blood perfusion, as for example the liver, the approximation does not hold at any wavelength. Furthermore, recent studies⁶⁻⁸ suggest that diffusion theory fails to describe light propagation in void-like regions, such as the ventricles in the brain.

When diffusion theory is not applicable other methods have to be used to calculate the propagation of photons in highly scattering media. For example, several researchers applied Monte Carlo simulations to determine the limits of diffusion theory.³⁻⁵ However, these simulations are limited to small tissue volumes. To compute the photon propagation in large, optically dense organs, such as the brain or the breast, Monte Carlo simulations are impractical. The computation times easily exceed several weeks or month. A faster way of accurately calculating the light distribution in highly scattering media is given by finite-difference discrete-ordinate formulation of the transport equation. While this method for solving the transport equation for arbitrary media was introduced as early as 1950⁹ and finds wide range applications in various fields that deal with the transport equation¹⁰⁻¹², it has barely been used to describe photon propagation in tissues.

In previous studies we have compared results from a finite-difference discrete-ordinate code with analytical diffusion calculations for homogeneous media and simple heterogeneous geometries.^{6,7} We found that when the absorption is comparable to scattering, diffusion theory overestimates the absorption effects and that diffusion theory yields erroneous results for void-like spaces. Having gained some understanding from studying simple media, we turn in this work to more complex and realistic situations. Magnetic resonance images of the human head are used to generate maps of optical properties (absorption coefficient, μ_a , and reduced scattering coefficient, μ_s). These maps were input to finite-difference transport and diffusion codes. The results confirm qualitatively findings of earlier work on simpler geometries and provide quantitative information about differences of diffusion and transport theory in the human head. In addition we discuss in detail effects of light propagation in void-like structure as found especially in the brain.

2. METHODS

2.1. Transport and Diffusion Code

In this study we use a time-independent finite-difference transport code called DANTSYS. This code was originally developed by Alcouffe et al at the Los Alamos National Laboratory¹³⁻¹⁷ for studies involving neutron transport in nuclear materials. Recently, it has been adapted by Hielscher and Alcouffe^{6,7} for photon migration in tissues. As described in detail elsewhere⁶ this code iteratively solves the set of equations given by the discretization of the transport equation. In this iterative process the code first calculates the diffusion solution and in subsequent iterations makes correction until it reaches the transport solution within a specified convergence criteria. Therefore, the code provides besides the transport solution a diffusion solution.

2.2. MRI-generated Data

MRI can differentiate between fatty white matter, the more watery gray matter, the cerebrospinal-fluid-filled ventricles, the skull, the skin and blood. These different tissues and fluids appear in MRI scans with different intensities. One obtains an optical property map ($\mu_a(r)$, $\mu_s'(r)$), by assigning different optical properties to different intensity values. Fig. 1 shows such a segmented scan for a slice that is taken just above the eyebrows through a human head. For example, clearly visible are the butterfly like ventricles in the center, which are filled with cerebrospinal fluid (CSF). The optical properties chosen for the different tissues and fluids are representative values for light in the near-infrared (600-900 nm). We have for white matter^{19,20} $\mu_a = 0.1 \text{ cm}^{-1}$ and $\mu_s' = 12 \text{ cm}^{-1}$, gray matter¹⁹⁻²¹ $\mu_a = 0.15 \text{ cm}^{-1}$ and $\mu_s' = 6, \text{ cm}^{-1}$, CSF $\mu_a = 0.01$ and $\mu_s' = 0.1 \text{ cm}^{-1}$, skull²² $\mu_a = 0.05 \text{ cm}^{-1}$ and $\mu_s' = 16 \text{ cm}^{-1}$, skin²³ $\mu_a = 0.2 \text{ cm}^{-1}$ and $\mu_s' = 5 \text{ cm}^{-1}$, and whole blood^{24,25}: $\mu_a = 3.0 \text{ cm}^{-1}$ and $\mu_s' = 18 \text{ cm}^{-1}$. The spatial resolution of the scan and the finite-difference grid is 2 mm. We assumed a constant refractive index of 1.4 for all regions. The refractive index in tissue may only vary between 1.35 and 1.51.²⁶⁻³⁰ In earlier work we showed that these small variations result in negligible effects.²³

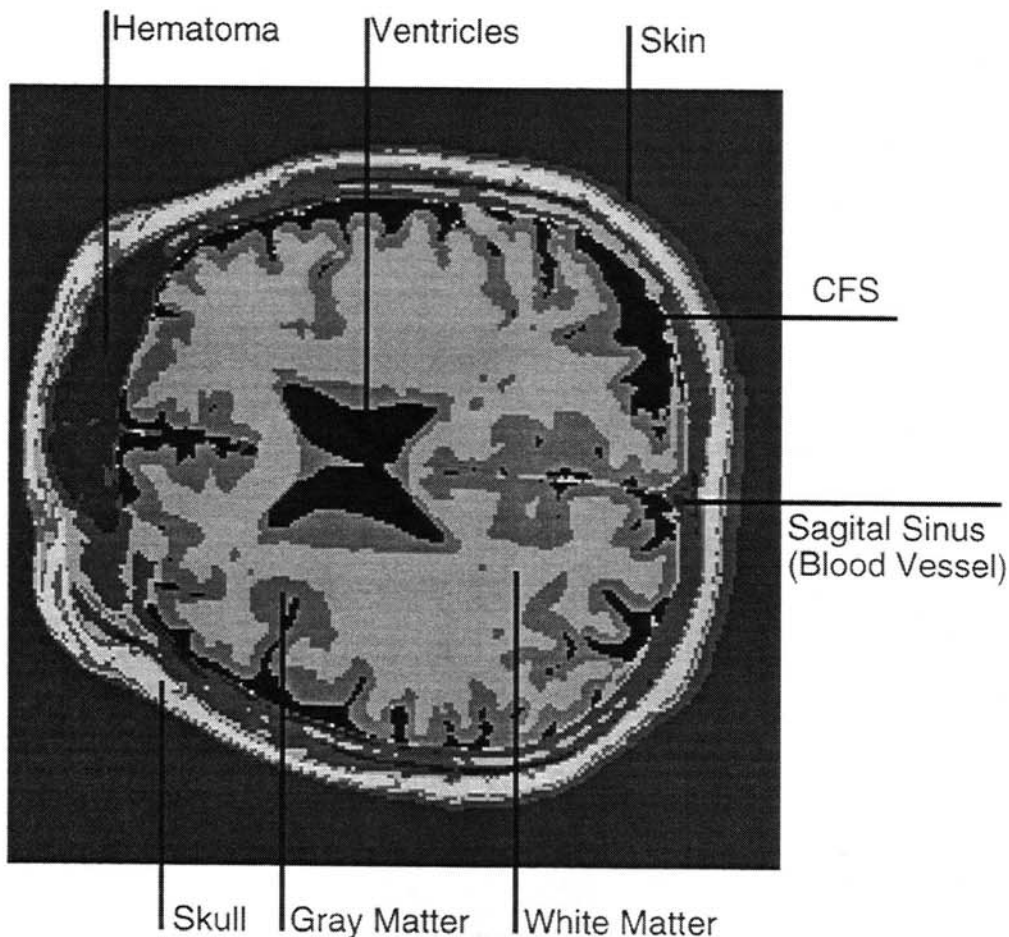


Fig. 1: Segmented 2D-MRI slice through human head just above the eyebrow.

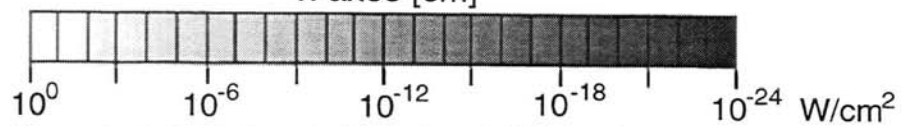
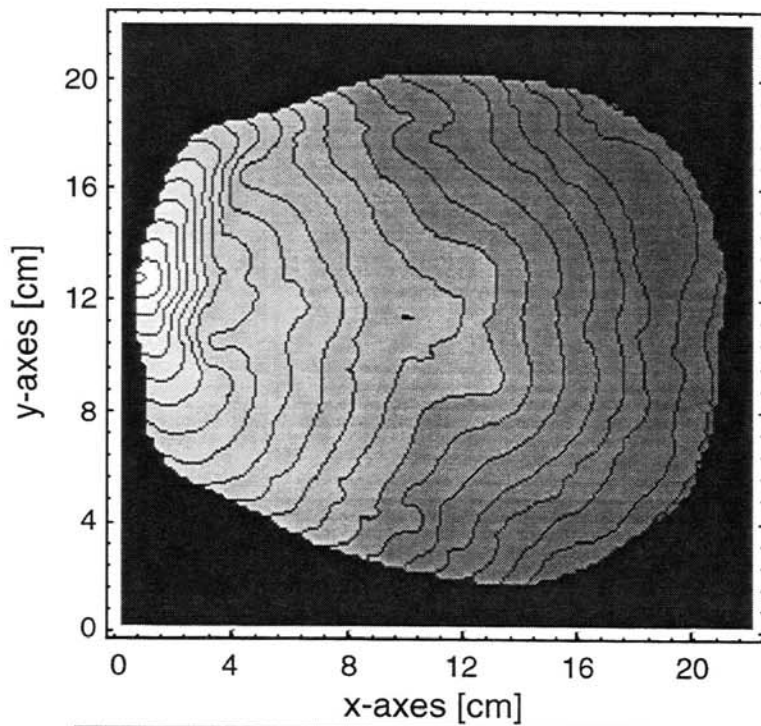
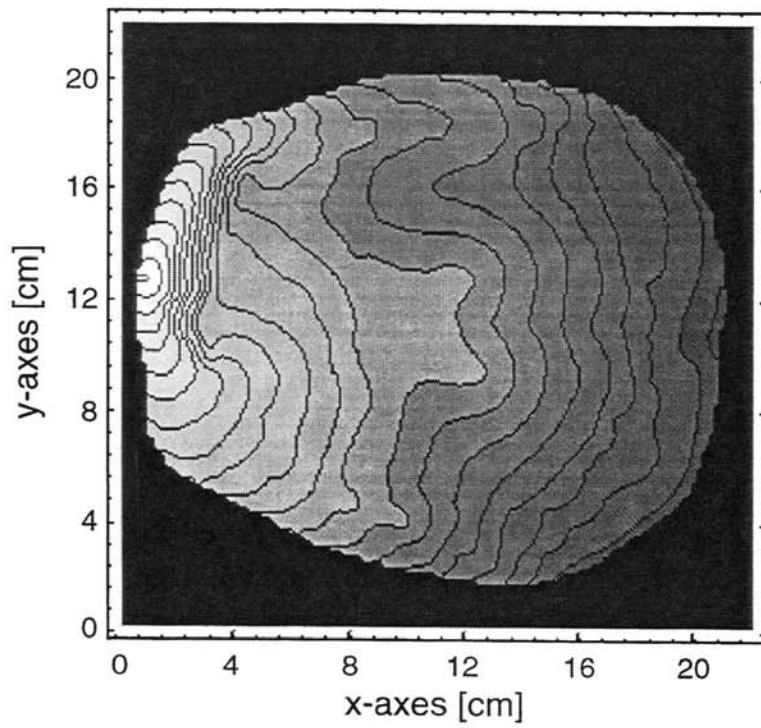


Fig. 2a,b: Calculation of the fluence in the head shown in Fig. 1: (a-top) Diffusion theory, (b-bottom) Transport theory. The pencil-beam light source is located at $x = 0.4$ cm, $y = 12.8$ cm. The iso-fluence lines indicate a drop of the fluence by one order of magnitude inbetween two lines.

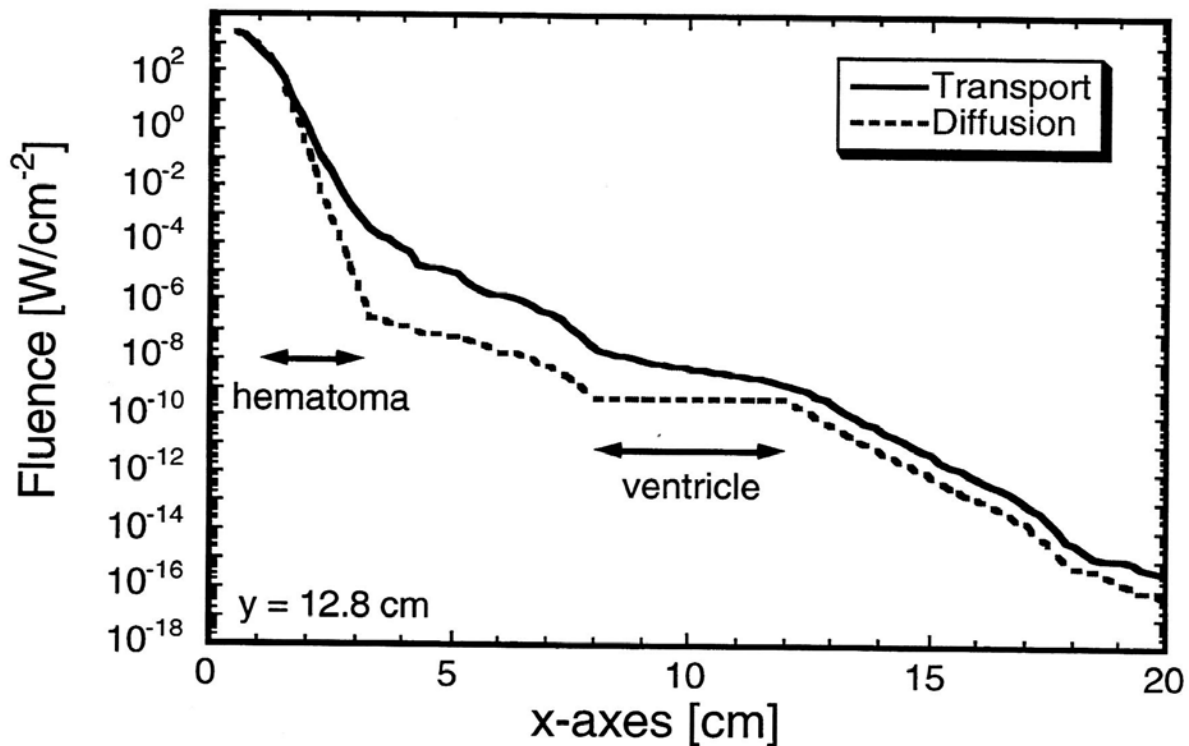


Fig. 3: Fluence in the head on a line ($0.4 \text{ cm} < x < 20.4 \text{ cm}$, $y = 12.8 \text{ cm}$) through Figs. 2a and 2b.

3. RESULTS

The results of the 2-dimensional finite-difference transport and diffusion simulations are shown in Figs. 2a and 2b. The light source is placed on the forehead ($x = 0.4 \text{ cm}$, $y = 12.8 \text{ cm}$) just above the hematoma. The different gray values represent different fluence levels. The iso-fluence lines indicate a drop of the fluence by one order of magnitude in between two lines. In the blood-filled region of the hematoma (approximately $2.5 \text{ cm} < x < 3.5 \text{ cm}$ and $11 \text{ cm} < y < 16.5 \text{ cm}$), the iso-fluence lines are much denser in the diffusion case than in the transport calculations. This indicates a much steeper decay of the fluence in this region when diffusion theory is used as compared to transport theory. Because in the hematoma μ_a is not much smaller than μ_s' , diffusion theory overestimates the absorption. This is in agreement with previously reported results on homogeneous media with high absorption.^{6,7}

Differences can also be observed in the void-like, CSF-filled region of the ventricles (approximately $8.5 \text{ cm} < x < 12.5 \text{ cm}$ and $8.5 \text{ cm} < y < 12.5 \text{ cm}$). Diffusion theory (Fig. 2a) predicts a decay of the fluence within the ventricles of less than one order of magnitude and the butterfly-like structure is clearly outlined in the 2D diffusion slice. Transport calculations (Fig. 2b) show a decay of over 2 orders of magnitude. Diffusion and transport results also differ in other CSF-filled regions, along $6 \text{ cm} < x < 16 \text{ cm}$, $y = 18 \text{ cm}$, and $7 \text{ cm} < x < 10 \text{ cm}$, $y = 4 \text{ cm}$. Compared to the transport solution, the fluence decays much slower along these "channels" of CSF when diffusion theory is used.

Rather than a 2D fluence map, Fig. 11 shows the fluence on the line ($0.4 \text{ cm} < x < 20.4 \text{ cm}$, $y = 12.8 \text{ cm}$) that contains the source and crosses through the hematoma and one of the ventricles. Clearly visible is the much faster decay of the fluence in the hematoma when diffusion theory is used. After the hematoma the diffusion calculations predict a fluence almost 3 orders of magnitude smaller than derived with transport theory. A reverse effect is observed in the void-like ventricle. Here diffusion theory underestimates the fluence decay.

4. DISCUSSION

The results of this study strongly suggest that the diffusion approximation to the Boltzmann transport equation is not applicable for studies of light propagation in the brain. The limitation is two fold: Firstly, trauma situation, where bleeding inside the brain occurs are not accurately described by diffusion theory. Secondly, void-like spaces can not be handled with diffusion theory. These regions are encountered in the ventricles of the brain and the subarachnoid space, which forms a boundary between the skull and the brain. Due to the convoluted nature of the brain, the thickness of the CSF-filled subarachnoid varies between about 1 and 10 mm. The effect of this layer for example on measurements of blood oxygenation in the brain has been subject of many discussions.^{8,23,31} Other void-like inclusion are for example the sinus cavities which are extensions of the nasal cavity.

The calculations on the MRI-generated data suggest that in void-like regions diffusion theory underestimates the decay of the fluence. To study this in more detail, we consider the following two simplified geometries. The first case (Fig. 4a) is a 120x120x120 mm cube with $\mu_s' = 5 \text{ cm}^{-1}$ and $\mu_a = 0.05 \text{ cm}^{-1}$, which encloses a 40x40x40 mm cube with $\mu_s' = 0.1 \text{ cm}^{-1}$ and $\mu_a = 0.001 \text{ cm}^{-1}$. A continuously-light-emitting point source is located inside the cube at 60 mm from the top and the bottom and 30 mm from one side. In the second example (Fig. 4b), we consider a 100x100mm square with $\mu_s' = 5 \text{ cm}^{-1}$ and $\mu_a = 0.05 \text{ cm}^{-1}$. The void-like structure ($\mu_s' = 0.1 \text{ cm}^{-1}$ and $\mu_a = 0.001 \text{ cm}^{-1}$) is this time a 4-mm-thick area, which surrounds an 84x84mm inner square. The point-source is centered on one side.

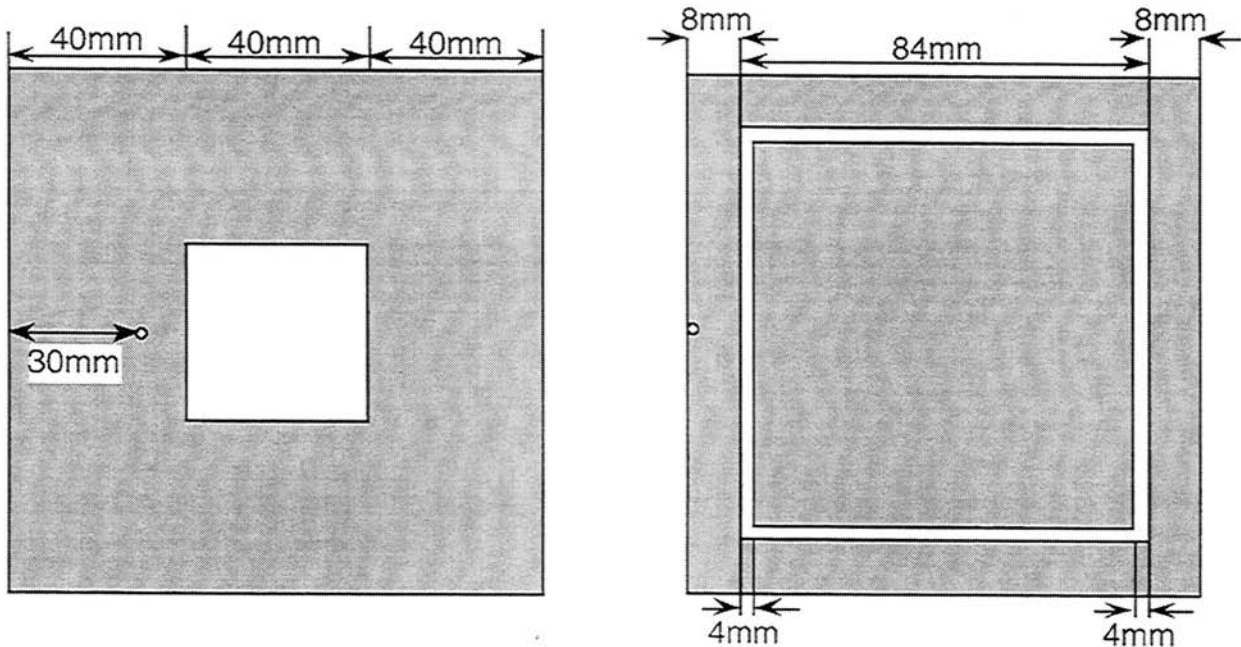


Fig. 4a,b: Geometries used in diffusion and transport simulations of void-like spaces. The voids ($\mu_s' = 0.1 \text{ cm}^{-1}$ and $\mu_a = 0.001 \text{ cm}^{-1}$) are white and the surrounding scattering media ($\mu_s' = 5 \text{ cm}^{-1}$ and $\mu_a = 0.05 \text{ cm}^{-1}$) are gray.

The result of the diffusion and transport calculations for the first case can be seen in Figs. 5a and 5b, respectively. Displayed is the fluence in a plane through the 3D cube, which contains the source. However, not the whole plane but only the result for the void is shown. Even though the diffusion approximation, $\mu_a/\mu_s \ll 1$, is valid in the void, differences between diffusion and transport theory occur. Transport theory predicts attenuation of fluence, while diffusion calculations result in almost constant fluence throughout the void. The transport solution can be understood as follows. In the void-like medium the fluence is highest at the point closest to the source. This point can be considered as a virtual point source for the void-like space. The fluence should attenuate even in the void-like space, due to geometrical effects. That is, in an absolute void the fluence decays inverse quadratically with distance from a point source. Transport theory can handle these void-like structures, while diffusion obviously can not.

The failure of diffusion theory to describe the light propagation in void-like spaces is even more apparent in the second example. Fig. 6a and 6b show the diffusion and transport simulations respectively for the case of void-like channels as depict in Fig. 4b. Big differences can be observed. Diffusion theory predicts light channeling within the almost clear

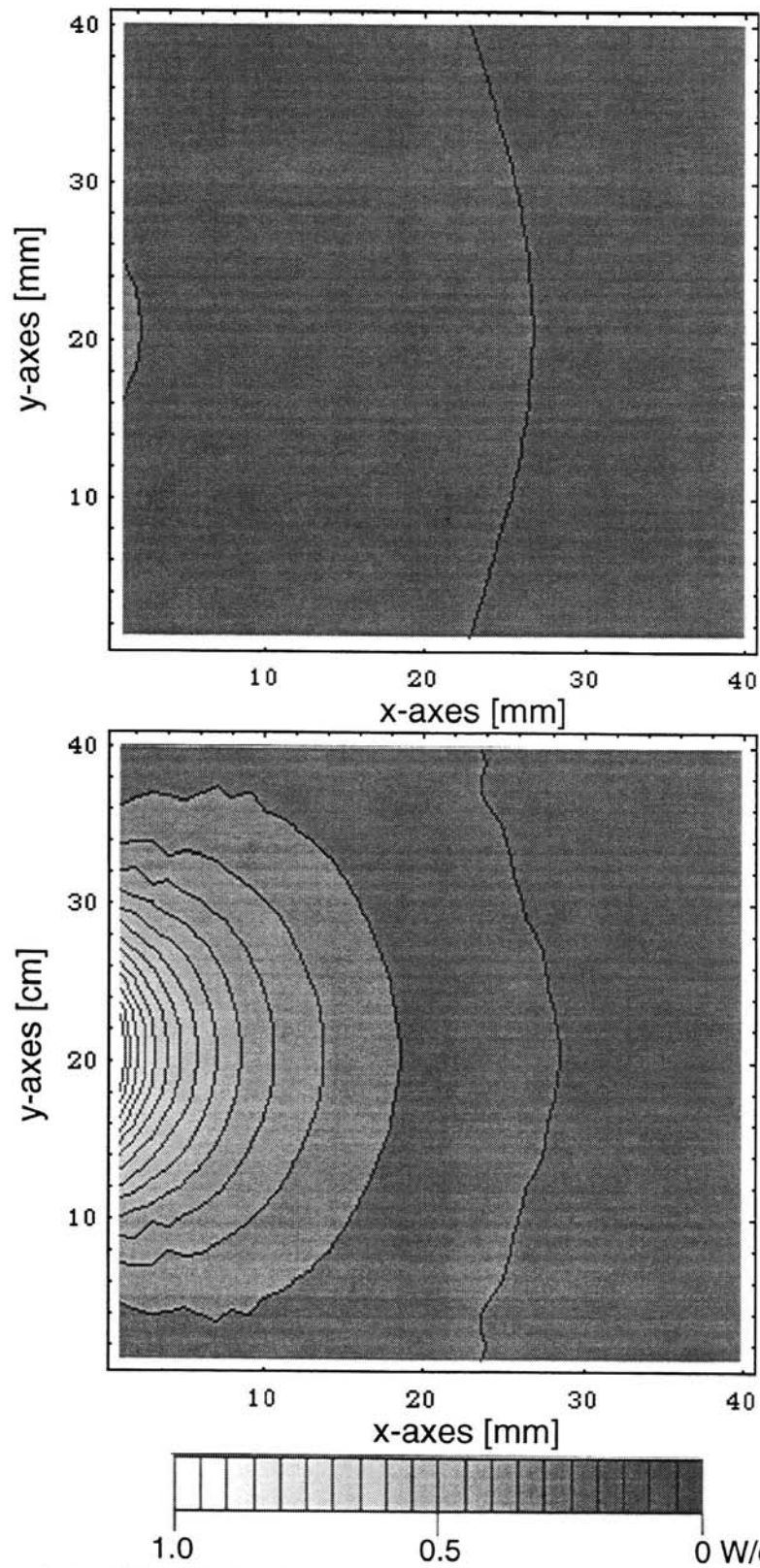


Fig. 5a,b: Fluence calculated by diffusion theory (a-top) and transport theory (b-bottom) for void-like geometry depicted in Fig. 4a. Cross sections displayed show only the 4x4 cm void-like region and not the surrounding medium.

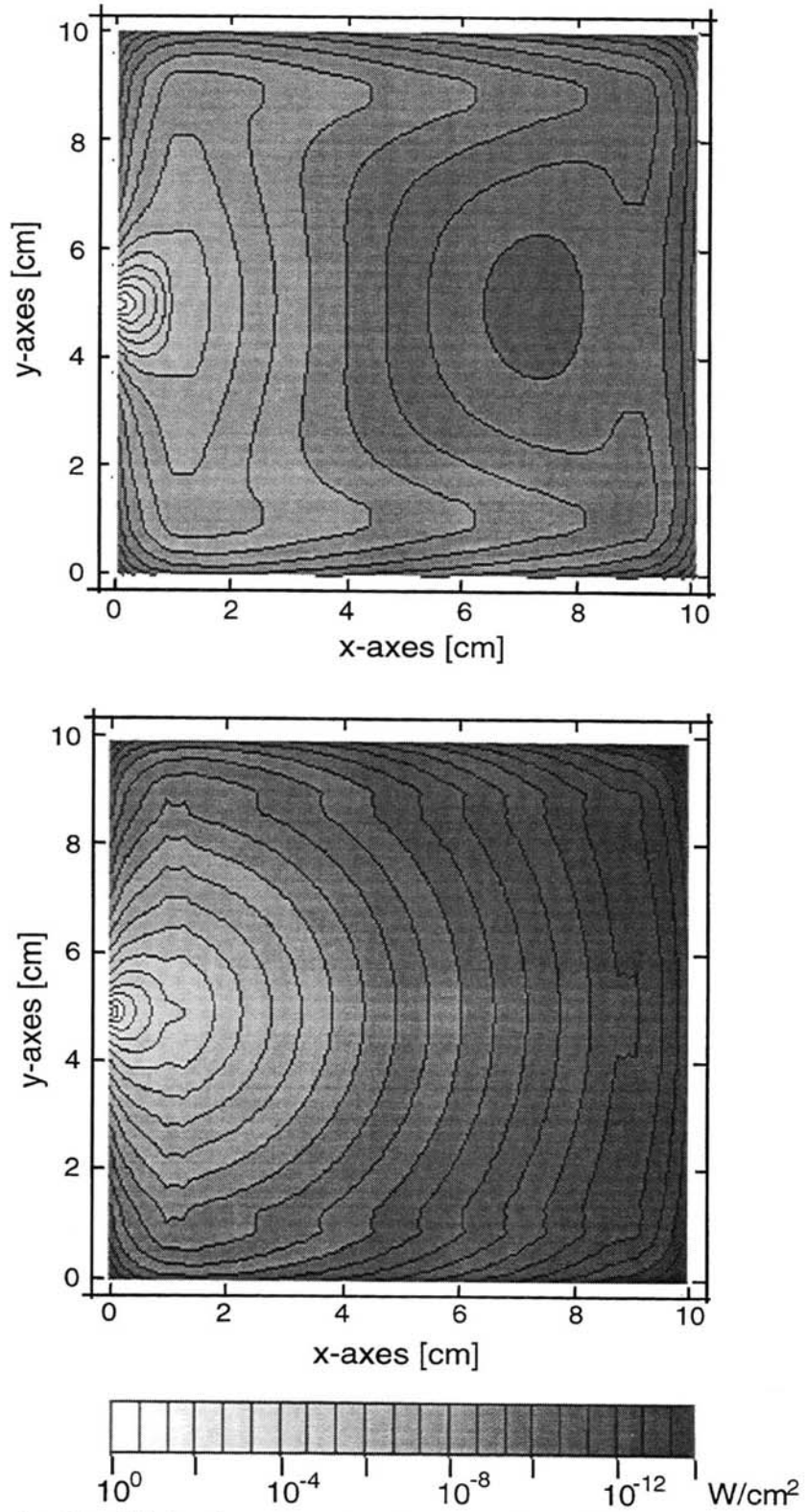


Fig. 6a,b: Fluence calculated by diffusion theory (a-top) and transport theory (b-bottom) for void-like geometry depicted in Fig. 4b.

space that surrounds the inner core. Transport theory calculations do not result in such channeling. As expected, the fluence decays even in these void-like channels due to geometrical effects. This results are in agreement with findings by Firbank et al⁸, who showed that diffusion theory predicts erroneous backreflections from a turbid media when a clear subsurface layer is introduced.

SUMMARY

We have developed a finite-difference discrete-ordinate algorithm that allows to calculate the transport as well as the diffusion solution for media with an arbitrary distribution of optical properties. In this work we presented results of calculations performed on MRI-generated data of brain tissue. Based on 2-dimensional MRI images we assigned optical properties to different regions of the brain. The finite-difference transport/diffusion code was then used to calculate the fluence. This allowed us to estimate the error caused by the diffusion approximation in realistic situations.

Our study shows that differences between transport and diffusion calculations occur especially in two regions. Diffusion theory fails to describe areas that are almost absorption and scattering free, such as the cerebrospinal-fluid-filled ventricles and the subarachnoid space. Furthermore, diffusion theory overestimates the absorption effect in media where the absorption is comparable to the scattering coefficient, such as hematoma.

ACKNOWLEDGMENTS

We liked to thank Prof. Yao Wang from the Department of Electrical Engineering at Polytechnic University, in Brooklyn, NY for the help in handling the MRI data. This work was supported in part by an NIH grant CA59955-CA61 and a fellowship from the director's office at Los Alamos National Laboratory.

REFERENCES

1. B. Tromberg, A. Yodh, E. Sevick, and D. Pine, "Diffusing photons in turbid media: introduction to the feature", *Appl. Opt.* **36**, pp. 9, 1997.
2. K.M. Yoo, F. Liu, and R.R. Alfano, "When does the diffusion approximation fail to describe photon transport in random media?", *Phys. Rev. Lett.* **64**, pp. 2647-2651, 1990.
3. S.J. Madsen, B.C. Wilson, M.S. Patterson, Y.D. Park, S.L. Jacques and Y. Hefetz, "Experimental tests of simple diffusion model for the determination of scattering and absorption-coefficients of turbid media from time-resolved diffuse reflectance measurements", *Appl. Opt.* **31** 3509-3517, 1992.
4. A.H. Hielscher, H. Liu, B. Chance, F.K. Tittel, and S.L. Jacques, "The influence of boundary conditions on the accuracy of diffusion theory in time-resolved reflectance spectroscopy of biological tissue", *Phys. Med. Biol.* **40**, pp. 1957-1975, 1995.
5. E. Okada, M. Schweiger, S.R. Arridge, M. Firbank, and D.T. Delpy, "Experimental validation of Monte-Carlo and finite-element methods for the estimation of the optical path-length in inhomogeneous tissues", *Applied Optics* **35** 3362-3371, 1996.
6. A.H. Hielscher, R.E. Alcouffe, "Non-diffusive photon migration in homogeneous and heterogeneous tissues," in *Photon Propagation in Tissue II*, B. Chance, D. Benaron, and G.J. Müller, eds., SPIE-The Internat. Society of Optical Engineering, Proc. 2925, pp. 22-30, 1996.
7. A.H. Hielscher, K.M. Hanson, R.E. Alcouffe, J.S. George, "Comparison of discrete ordinate and diffusion theory calculations for photon migration in heterogeneous tissues," OSA Trends in Optics and Photonics: Advances in Optical Imaging and Photon Migration, R.R. Alfano and J.G. Fujimoto, eds., Optical Society of America, Washington, DC, Vol. 2, pp. 55-59, 1996.
8. M. Firbank, S.R. Arridge, M. Schweiger, and D.T. Delpy, "An investigation of light transport through scattering bodies with non-scattering regions", *Physics in Medicine and Biology* **41**, 767-783, 1996.
9. S. Chandrasekhar, *Radiative Transfer*, Academic Press, New York, NY, 1950.
10. K.N. Liou, "A numerical experiment on Chandrasekhar's discrete-ordinate method for radiative transfer: applications to cloudy and hazy atmospheres", *J. Atmos. Sci.* **30**, pp. 1303-1326, 1973.
11. W.A. Rhoades and R.L. Childs, "A 3-Dimensional discrete ordinates neutron photon transport code", *Nuclear Science and Engineering* **107**, pp. 397-398, 1991.
12. A. Badruzzaman and J. Chiaramonte, "A comparison of Monte Carlo and discrete ordinates methods in a 3-dimensional well-logging problem", *Trans. Am. Nucl. Soc.* **50**, pp. 265-267, 1985.
13. R.E. Alcouffe, "Diffusion synthetic acceleration: Method for the diamond-differenced discrete-ordinates equation", *Nuc. Sci. Eng.* **64**, pp. 344-352, 1977.

14. R.E. Alcouffe and R.D. O'Dell, *Transport Calculation for Nuclear Analyses: Theory and Guidelines for Effective Use of Transport Codes*, Los Alamos National Laboratory, Los Alamos, NM: Report LA-10983-MS, 1987.
15. R.E. Alcouffe, "A diffusion accelerated S_N transport method for radiation transport on a quadrilateral mesh", *Nuc. Sci. Eng.* **105**, pp. 191-197, 1990.
16. R.E. Alcouffe, "An adaptive weighted diamond differencing method for three-dimensional xyz geometry", *Trans. Am. Nuc. Soc.* **68** Part A, pp. 206-212, 1993.
17. R.E. Alcouffe, R.S. Baker, F.W. Brinkley, D.R. Marr, R.D. O'Dell, and W.F. Walters, *DANTSYS: A Diffusion Accelerated Neutral Particle Transport Code System*, Los Alamos National Laboratory, Los Alamos, NM: Manual LA-12969-M, 1995.
18. E.M. Sevick and B. Chance, "Photon Migration in a model of the head measured using time- and frequency-domain techniques: potential of spectroscopy and imaging", in *Time-Resolved Spectroscopy and Imaging of Tissue*, B. Chance, ed., SPIE-The International Society of Optical Engineering, Proc. 1431 pp. 84-96, 1991.
19. E.M. Sevick, B. Chance, J. Leigh, S. Nioka, and M. Maris, "Quantitation of Time- and Frequency-Resolved optical spectra for the determination of tissue oxygenation", *Analytical Biochemistry* **195**, pp. 330-351, 1991.
20. P. van der Zee, M. Essenpreis, and D.T. Delpy, "Optical properties of brain tissue", in *Photon Migration and Imaging in Random Media and Tissues*, B. Chance B, R.R. Alfano, and A. Katzir, eds., SPIE-The International Society of Optical Engineering, Proc. 1888, pp. 454-465, 1992.
21. F. Bevilacqua, P. Marquet, C. Depeursinge, and E.B. de Haller, "Determination of reduced scattering and absorption coefficients by a single charge-coupled-device array measurement, part II: measurements on biological tissue", *Optical Engineering* **34**, pp. 2064-2069, 1995.
22. M. Firbank, M. Hiraoka, M. Essenpreis and D.T. Delpy, "Measurement of the optical properties of the skull in the wavelength range 650-950nm", *Phys Med Biol* **38**, pp. 503-510, 1993.
23. A.H. Hielscher, H. Liu, B. Chance, F.K. Tittel, and S.L. Jacques, "Time-resolved photon emission from layered turbid media", *Applied Optics* **35**, pp. 719-728, 1996.
24. H. Liu, A.H. Hielscher, B. Chance, S.L. Jacques, and F.K. Tittel, "Influence of blood vessels on the measurements of hemoglobin oxygenation as determined by time-resolved reflectance spectroscopy", *Medical Physics* **22**, pp. 1209-1217, 1995.
25. A.M. Nilsson, G.W. Lucassen, W. Verkruyse, S. Andersson-Engels, and M.J.C. Van Gemert, "Changes in optical properties of human whole blood in vitro due to slow heating", *Photochemistry and Photobiology*, in press
26. A. Brunsting and P. F. Mullaney, "Differential light scattering from spherical mammalian cells," *Biophysics J.* **14**, pp. 439-453, 1974.
27. S. Fujime, M. Takasaki-Oshito, and S. Miyamoto, "Dynamic light scattering from polydisperse suspensions of large spheres," *Biophys. J.* **54**, pp. 1179-1184, 1988.
28. *CRC Handbook of Chemistry and Physics*, 70th ed., R.C. Weast, ed., CRC Press, Cleveland, OH, 1989.
29. F. A. Duck, *Physical Properties of Tissue*, Academic, London, 1990, p.63.
30. H. Li and S. Xie, "Measurement method of the refractive index of biotissue by total internal reflection," *Applied Optics* **35**, pp. 1793-1795, 1996.
31. A.H. Hielscher, H. Liu, B. Chance, F.K. Tittel, and S.L. Jacques, "Phase resolved reflectance spectroscopy on layered turbid media", in *Optical Tomography, Photon Migration, and Spectroscopy of Tissue and Model Media: Theory, Human Studies, and Instrumentation*, B. Chance, R. Alfano, eds., SPIE-The International Society of Optical Engineering, Proc. 2389: Part 1, pp. 248-256, 1995.